Eur. Phys. J. Special Topics **216**, 57–71 (2013)

DOI: 10.1140/epjst/e2013-01729-y

THE EUROPEAN PHYSICAL JOURNAL SPECIAL TOPICS

Regular Article

Optimal least-squares estimators of the diffusion constant from a single Brownian trajectory

Denis Boyer[1], David S. Dean[2], Carlos Mejía-Monasterio[3,4,a], and Gleb Oshanin[5]

[1] Instituto de Física, Universidad Nacional Autónoma de México, D.F. 04510, Mexico
[2] Université de Bordeaux and CNRS, Laboratoire Ondes et Matière d'Aquitaine (LOMA), UMR 5798, 33400 Talence, France
[3] Laboratory of Physical Properties, Technical University of Madrid, Av. Complutense s/n, 28040 Madrid, Spain
[4] Department of Mathematics and Statistics, University of Helsinki, PO Box 68, 00014 Helsinki, Finland
[5] Laboratoire de Physique Théorique de la Matière Condensée (UMR CNRS 7600), Université Pierre et Marie Curie/CNRS, 4 place Jussieu, 75252 Paris Cedex 5, France

Received 30 November 2012 / Received in final form 6 December 2012
Published online 31 January 2013

Abstract. Modern developments in microscopy and image processing are revolutionising areas of physics, chemistry, and biology as nanoscale objects can be tracked with unprecedented accuracy. However, the price paid for having a direct visualisation of a single particle trajectory with high temporal and spatial resolution is a consequent lack of statistics. This naturally calls for reliable analytical tools which will allow one to extract the properties specific to a statistical ensemble from just a single trajectory. In this article we briefly survey different analytical methods currently used to determine the ensemble average diffusion coefficient from single particle data and then focus specifically on weighted least-squares estimators, seeking the weight functions for which such estimators are ergodic. Finally, we address the question of the effects of disorder on such estimators.

1 Introduction

Single particle tracking (SPT) can be traced back to the classic studies of Jean Baptiste Perrin on Brownian motion [1,2]. With the advent of modern experimental techniques, recent years witnessed an explosion of different approaches aiming at probing physical and biological processes at the level of a single molecule. A SPT experiment uses computer-enhanced video microscopy to generate the time series of the position $r_1,\ r_2,\ \ldots,\ r_N$ at times $t_1,\ t_2,\ \ldots,\ t_N$, of an individual particle trajectory in a medium, (see, e.g., [3,4]). Properly interpreted, the information drawn from a single, or a finite number of trajectories, provides insight into the mechanisms

[a] e-mail: carlos.mejia@helsinki.fi

and forces that drive or constrain the motion of the particle. Nowadays, single particle tracking is extensively used to characterise the microscopic rheological properties of complex media [5], and to probe the active motion of biomolecular motors [6]. In biological cells and complex fluids, SPT methods have become instrumental in demonstrating deviations from normal Brownian motion of passively moving particles (see, e.g., [7–11]).

The reliability of the information drawn from SPT analysis, obtained at high temporal and spatial resolution but at expense of statistical sample size, is not always clear. Time averaged quantities associated with a given trajectory are usually subject to large trajectory-to-trajectory fluctuations even for simple diffusion. For proteins transported in the cell cytoplasm or molecules in aqueous environments in general, Brownian diffusion is the basic transport mechanism [12]. Notwithstanding that diffusion is ubiquitous in nature, recent studies have suggested that transport on cell's membrane [13], as well as in the cytoplasm [11], may not be limited to pure diffusion, although the microscopic origin of anomalous diffusion remains unclear. For a wide class of anomalous diffusions, described by continuous-time random walks, time-averages of certain particle's observables are, by their very nature, themselves random variables distinct from their ensemble averages [14,15]. For example, the square displacement time-averaged along a given trajectory differs from the ensemble averaged mean squared displacement[15–17]. By analyzing time-averaged displacements of a particular trajectory realization, subdiffusive motion can actually look normal, although with strongly differing diffusion coefficients from one trajectory to another [15–17] and showing substantial ageing effects [18]. Conflicting results in the identification of the underlying transport mechanisms and their characterization has generated in recent years a debate on the most appropriate methodology for the determination of the diffusion coefficient from SPT data.

Even though standard Brownian motion is much better understood than anomalous diffusion, the analysis of its trajectories is far from being as straightforward as one might think, and all the above-mentioned troublesome problems persist. For instance, in bounded systems, substantial manifestations of trajectory-to-trajectory fluctuations in the first passage time phenomena have been recently revealed [19,20].

Standard fitting procedures applied to long but finite d-dimensional Brownian trajectories unavoidably lead to fluctuating estimates D_f of the diffusion coefficient, which might be very different from the true ensemble average value D,

$$D = \frac{\mathbb{E}\left[\mathbf{B}_t^2\right]}{2dt}. \tag{1}$$

Using different fitting procedures, variations by orders of magnitude have been observed in SPT measurements of the diffusion coefficient for diffusion of the LacI repressor protein along elongated DNA [21], in the plasma membrane [4] or for diffusion of a single protein in the cytoplasm and nucleoplasm of mammalian cells [22]. The dispersion of D_f observed from different single particle trajectories results from the rather complex environments in which the measurements are performed. Each trajectory will have its own thermal history, particle interactions with different impurities, etc. Moreover, the broad histograms for observed D can also be due to blur and localization errors, intrinsic of any experimental measurements, as discussed in [23–26].

The broad dispersion of diffusion constant estimates extracted from SPT analysis raises several important questions: Does an optimal methodology able to determine the diffusion coefficient from just one single-particle trajectory exist? If the answer to this question is positive, then what is the performance of such methodology given the finite length and finite time resolution of the measured trajectory? Clearly, it is highly desirable to have a reliable estimator even for the hypothetical pure cases,

such as, e.g., unconstrained standard Brownian motion. Such an estimator must possess an ergodic property so that its most probable value should converge to the ensemble average and the variance should vanish as the observation time increases.

This is often not the case and moreover, ergodicity of a given estimator is not known *a priori* and has to be tested for each particular form of the estimator. Moreover, the knowledge of the distribution of such an estimator could provide a useful gauge to disentangle the effects of the medium complexity as opposed to variations in the underlying thermal noise driving microscopic diffusion. Recently, much effort has been invested in the analysis of this challenging problem and several important results have been obtained for the estimators based on the time-averaged mean-square displacement [27–29], mean maximal excursion [30], or the maximum likelihood approximation [23,31,32].

In this paper we first review, in Sect. 2, some of the existing statistical methodologies used to extract the diffusion coefficient of single-particle Brownian trajectories. In Sect. 3, we focus on a family of weighted least-squares estimators based on single-time averages that we have recently introduced, and in Sect. 4, we obtain the distribution function of the estimate D_f and study its ergodic properties. When the underlying dynamics is not Brownian, the ergodicity properties of the weighted least-squares estimators is not guaranteed. As shown in Sect. 5, where we present new results on the estimation of the diffusion coefficient of a Brownian particle moving on a random correlated potential. Sect. 6 contains our final remarks.

2 Estimating the diffusion coefficient of single trajectories

Consider a d-dimensional Brownian process $\mathbf{B}_t$ with variance $\mathrm{Var}\,[\mathbf{B}_t] = 2dDt$, and D as defined in Eq. (1).

We start this section by considering a simple-minded, rough estimate of D_f, defining it as the slope of the line connecting the starting and the end-points $\mathbf{B}_t$ of a given trajectory, namely $D_f = \mathbf{B}_t^2/2dt$. By definition $\mathbb{E}\,[D_f] = D$. A single trajectory diffusion coefficient D_f so defined is a random variable whose probability density function $P(D_f)$ is the so-called chi-squared distribution with d degrees of freedom, namely

$$P(D_f) = \frac{1}{\Gamma(d/2)} \left(\frac{d}{2D}\right)^{d/2} D_f^{d/2-1} \exp\left(-\frac{d}{2} \cdot \frac{D_f}{D}\right), \tag{2}$$

where $\Gamma(\cdot)$ is the Gamma-function. Clearly this distribution diverges as $D_f \to 0$ for $d = 1$, $P(0)$ is constant for $d = 2$, and only for $d > 2$ the distribution has a bell-shaped form with the finite most probable value $D_f^* = (1 - 2/d)D$. This means that, e.g., for $d = 3$, the most likely value extracted from a single Brownian trajectory is only $D_f = D/3$.

A more refined method, known as Least-Squares Estimator (LSE), than the previous one consists in taking not only the starting and end-points, but the least-squares estimate of the trajectory in the full time interval, say $t \in [0, T]$, namely

$$F_{\mathrm{LSE}} = \int_0^T \left(\mathbf{B}_t^2 - l(t)\right)^2 dt, \tag{3}$$

where in the simplest case, the dynamical law is taken as $l(t) = 2dD_{\mathrm{LSE}}t$. Minimizing (3) with respect to D_{LSE} we obtain the LSE as

$$D_{\mathrm{LSE}} = \frac{3}{8dT^3} \int_0^T \mathbf{B}_t^2 t dt. \tag{4}$$

Another related method, commonly used in the analysis of SPT, experimental data consists in the least-squares fitting of the time-averaged square displacement, also called Mean Square Displacement (MSD) [4,12,22]. For a trajectory followed through a time interval T, this is defined as

$$F_{\mathrm{MSD}}(t) = \frac{1}{T-t}\int_0^{T-t} \left(\mathbf{B}_{t+s} - \mathbf{B}_s\right)^2 ds. \tag{5}$$

At short time lags $t \to 0$, the time average F_{MSD} coincides with the ensemble average $\mathbb{E}\left[\mathbf{B}_t^2\right]$, due to the ergodicity of the diffusion processes. However, due to the finite length of experimental trajectories, the MSD analysis (5), is performed over a large fraction of intervals t, even when it is clear that the small-t behaviour is often restricted only to a very small interval compared to the total duration of the trajectory [31]. Replacing $\mathbf{B}_t^2$ by the MSD trajectory F_{MSD} in Eq. (3) we obtain for a linear dynamical law the MSD estimator

$$D_{\mathrm{MSE}} = \frac{3}{8dT^3}\int_0^T F_{\mathrm{MSD}}(t)t\, dt. \tag{6}$$

Calculating the MSD is one of the most popular methods for the analysis of SPT experimental data. However, this method presents a number of fundamental limitations, leading to non reliable estimations of the diffusion coefficient [26]. Some of these limitations can be improved by considering weighted MSE, with a time dependent weight that takes into account the growth of the variance in time [12]. Other limitations are rooted to the fact that, differently than the LSE, the MSD estimator is a two-time function. This fact renders the MSD estimator particularly fragile with respect to the localization errors intrinsic to the experimental acquisition of the data. This fragility has been only recently recognized and studied by several authors (see *e.g.* [23–26]). With no additional errors, the ensemble average of (5), *i.e.*, the average of Eq. (5) over infinitely different trajectories, coincides with $\mathbb{E}\left[\mathbf{B}_t^2\right]$ [33]. However, in experimental data, the position of the particle at any given time is acquired during a finite integration time, yielding a static localization error δ. Since, the localization error involves the unknown diffusion coefficient D, the ensemble average of Eq. (5) is modified as [34]

$$\mathbb{E}\left[F_{\mathrm{MSD}}(t)\right] = 2\left(dDt + \delta^2\right). \tag{7}$$

Additional dynamic errors due to motion blur reduce the previous expression by $2D\tau/3$, where τ is the time interval at which the position of the particle is recorded [35]. Full consideration of these errors and modeling of the motion blur has been recently studied in [23–25], and in [26] an optimized version of the least-squares fitting for the MSD has been proposed. The authors of [26] showed as well that the variance of this optimized MSE decays inversely proportional to the length of the trajectory, which means that for very long trajectories, the estimated value of the diffusion constant becomes trajectory independent. Therefore, this two-time estimator is ergodic.

A conceptually different fitting procedure has been discussed in [31] which amounts to maximizing the unconditional probability of observing the whole trajectory $\mathbf{B}(t)$, assuming that it is drawn from a Brownian process with mean-square displacement $2dDt$. This is the maximum likelihood estimate which takes the value of D that maximizes the likelihood of $\mathbf{B}(t)$, defined as:

$$L_T = \prod_{t=0}^{T} (4\pi Dt)^{-d/2} \exp\left(-\frac{\mathbf{B}_t^2}{4Dt}\right). \tag{8}$$

Minimization of the logarithm of L_T with respect to D yields the Maximum Likelihood Estimator (MLE) for the diffusion coefficient of a Brownian trajectory as [31]

$$D_{\mathrm{MLE}} = \int_0^T \frac{\mathbf{B}_t^2}{t}\, dt. \tag{9}$$

This estimator was studied in [31] in one dimension, and it was shown that the MLE is superior to those based on the LS unweighted minimization. As a matter of fact, the distribution of D_{MLE} not only appears narrower than the distribution of D_{LSE}, resulting in a smaller dispersion, but also the most probable value of the diffusion coefficient appears closer to the ensemble average D [31]. More recently, the same conclusions were obtained in [32] for arbitrary dimensions.

3 Weighted least-squares estimators of the diffusion coefficient

In a recent paper [36], we have studied a family of least-squares one-time estimators defined as

$$u_\alpha = \frac{A_\alpha}{T} \int_0^T \omega(t)\, \mathbf{B}_t^2\, dt, \tag{10}$$

where $\omega(t)$ is the weighting function of the form

$$\omega(t) = \frac{1}{(t_0 + t)^\alpha}\,, \tag{11}$$

α being a tunable exponent (positive or negative), t_0 – a lag time and A_α – the normalization constant, appropriately chosen in such a way that $\mathbb{E}\{u_\alpha\} \equiv 1$, so that

$$A_\alpha = \frac{T}{2dD} \left(\int_0^T \frac{t\, dt}{(t_0 + t)^\alpha} \right)^{-1}. \tag{12}$$

Such a normalization permits a direct comparison of the effectiveness of estimators corresponding to different values of α.

The estimator u_α in Eq. (10) minimizes the least-squares functionals with a weighting function $\omega(t) = (t_0 + t)^{-\alpha}$. Consider a d-dimensional trajectory $\mathbf{B}_t$ with $t \in [0, T]$. To estimate the diffusion coefficient D_F from this trajectory, one writes the least-squares functional of the form

$$F = \frac{1}{2} \int_0^T \frac{\omega(t)}{t} \left(\mathbf{B}_t^2 - 2dD_F t \right)^2 dt\,, \tag{13}$$

and seeks to minimize it with respect to the value of D_F, considered as a variational parameter. Eq. (13) is a generalized weighted least-squares functional, with a certain weighting function $\omega(t)$, which depending on whether it is a decreasing or an increasing function of t, will emphasize the short time or the long time behavior of the trajectory $\mathbf{B}_t$, respectively.

After minimization of F with respect to D_F we find that

$$\frac{D_F}{D} = \left(\frac{1}{T} \int_0^T dt\, \omega(t)\, \mathbf{B}_t^2 \right) \left(\frac{2dD}{T} \int_0^T dt\, t\, \omega(t) \right)^{-1}. \tag{14}$$

Finally, identifying the denominator with the normalization A_α and choosing $\omega(t) = (t_0 + t)^{-\alpha}$, we recover our definition (10). Furthermore, note that $\alpha = -1$ corresponds

to the unweighted LSE and $\alpha = 1$ corresponds to MLE defined in the previous section. Therefore, our generalized estimate (10), possesses a nice property to contain, as particular cases, two other commonly used estimators.

For standard Brownian motion, the lag time t_0, corresponding to the time at which the measurement is started, can be set equal to zero. However, it is useful to keep the explicit dependence on t_0 since it is equal to the resolution ϵ at which an experimental trajectory is recorded as $\epsilon = t_0/T$. Moreover, in [32] it was found that for anomalous diffusion, or for Brownian motion in presence of disorder, t_0 plays a significant role.

In [36], we have studied the family of estimators (10), and determined a unique value of α for which u_α is ergodic, so that the single trajectory diffusion coefficient $D_F \to D$ as $\epsilon = t_0/T \to 0$. In the next section we briefly sketch the derivation of the probability distribution function $P(u_\alpha)$ and discuss its properties.

4 Distribution of the weighted estimators

The fundamental characteristic property to derive the probability distribution function $P(u_\alpha)$ is the moment-generating function $\Phi(\sigma)$ of the random variable in Eq. (10) defined as

$$\Phi(\sigma) = \mathbb{E}\left[\exp\left(-\sigma u_\alpha\right)\right], \tag{15}$$

where σ is positive definite parameter, $0 \leq \sigma < \infty$.

Using the fact that a d-dimensional Brownian motion can be decomposed into a product of its d one-dimensional components, the generating function can be written as

$$\Phi(\sigma) = G(\sigma)^d = \left(\mathbb{E}\left[\exp\left(-\frac{\sigma A_\alpha}{T}\int_0^T \omega(\tau)\, B_\tau^2(i)\, d\tau\right)\right]\right)^d. \tag{16}$$

Following [31,32], we introduce an auxiliary functional

$$\Psi(x,t) = \mathbb{E}_t^x\left\{\exp\left(-\frac{\sigma A_\alpha}{T}\int_t^T \omega(\tau)\, B_\tau^2\, d\tau\right)\right\}, \tag{17}$$

where the expectation is for a Brownian motion starting at x at time t. Clearly, $G(\sigma) = \Psi(0,0)$. This functional satisfies the Feynman-Kac type formula

$$\Psi(x,t) = \mathbb{E}_{dB}\left\{\Psi(x+dB_t, t+dt)\left(1 - \frac{\sigma A_\alpha \omega(t)}{T}x^2 dt\right)\right\}, \tag{18}$$

where dB_t is an infinitesimal Brownian increment such that $\mathbb{E}_{dB}\{dB_t\} = 0$ and $\mathbb{E}_{dB}\{dB_t^2\} = 2Ddt$, and $\mathbb{E}_{dB}$ denotes averaging with respect to the increment dB_t. Furthermore, expanding the right-hand-side of the latter equation to second order in dB_t, linear order in dt and performing averaging, we find that $\Psi(x,t)$ obeys the Schrödinger like equation with a harmonic, time-dependent potential

$$\frac{\partial \Psi(x,t)}{\partial t} = -D\frac{\partial^2 \Psi(x,t)}{\partial x^2} + \frac{\sigma A_\alpha \omega(t)}{T}x^2 \Psi(x,t), \tag{19}$$

subject to boundary condition $\Psi(x,T) = 1$ for any x.

The solution of Eq. (19), and thus of the generating function (16), was explicitly obtained in [36] for $\alpha = 2$ and $\alpha \neq 2$. In the latter case, the moment-generating function, to leading order in $\epsilon = t_0/T$, is given by:

$$\Phi(\sigma) = \left[\Gamma(\nu) \left(\frac{\sigma}{\chi_1}\right)^{\frac{1-\nu}{2}} \mathrm{I}_{\nu-1}\left(2\sqrt{\frac{\sigma}{\chi_1}}\right) \right]^{-d/2}, \quad \text{for} \quad \alpha < 2, \tag{20}$$

$$\Phi(\sigma) = \left[\Gamma(1-\nu) \left(\frac{\sigma}{\chi_2}\right)^{\frac{\nu}{2}} \mathrm{I}_{-\nu}\left(2\sqrt{\frac{\sigma}{\chi_2}}\right) \right]^{-d/2}, \quad \text{for} \quad \alpha > 2, \tag{21}$$

where $\nu = 1/(2-\mu)$, $I_\mu(z)$ is the modified Bessel function [39] and

$$\chi_1 = \frac{d(2-\alpha)}{2} \quad \text{and} \quad \chi_2 = \frac{d(\alpha-2)}{2(\alpha-1)}. \tag{22}$$

For the particular case of $\alpha = 2$, we find that the moment-generating function is given for arbitrary ϵ explicitly by

$$\Phi(\sigma) = \left\{ \frac{(\delta+1)}{2\delta\epsilon^{(\delta-1)/2}} \left[\left(1 + \frac{\delta-1}{\delta+1}\epsilon^\delta\right) \cosh\left(\sqrt{2a\xi\sigma}\right) + \frac{\delta-1}{2\sqrt{2a\xi\sigma}} \left(1+\epsilon^\delta\right) \sinh\left(\sqrt{2a\xi\sigma}\right) \right] \right\}^{-d/2}. \tag{23}$$

First we focus on the variance of the estimator given in (10). The variance $\mathrm{Var}(u_\alpha)$ is obtained by differentiating Eqs. (20) or (21) twice with respect to σ and setting σ equal to zero. For arbitrary $\alpha \neq 2$ the variance to leading order in ϵ is then given explicitly by

$$\mathrm{Var}\left[u_\alpha\right] = \frac{2}{d} \begin{cases} (2-\alpha)/(3-\alpha), & \alpha < 2, \\ (\alpha-2)/(2\alpha-3), & \alpha > 2. \end{cases} \tag{24}$$

The result in the latter equation is depicted in Fig. 1 and shows that, strikingly, the variance can be made arbitrarily small in the leading in ϵ order by taking α gradually closer to 2, either from above or from below. The slopes at $\alpha = 2^+$ and $\alpha = 2^-$ appear to be the same, so that the accuracy of the estimator will be the same when approaching $\alpha = 2$ from above or below. Equation (24), although formally invalid for $\alpha = 2$, also suggests that the estimator in Eq. (10) with $\alpha = 2$ possesses an ergodic property.

A word of caution is now in order. Finite-ϵ corrections to the result in Eq. (24) are of order of $\mathcal{O}(\epsilon^{2-\alpha})$ for $1 < \alpha < 2$, which means that this asymptotic behavior can be only attained when $\epsilon \ll \exp\left(-1/(2-\alpha)\right)$. In other words, in principle, the variance can be made arbitrarily small by choosing α closer to 2, but only at expense of increasing either the experimental resolution or the observation time T, which is clearly seen in Fig. 1.

The solid circles in Fig. 1 correspond to numerical results of random walks on a 3-dimensional lattice and computed $P(u_\alpha)$ using Eq. (10) from a large ensemble of trajectories, for different values of α and different resolution ϵ. For $\alpha < 1.5$ or $\alpha > 2.5$, the variance computed numerically is well described by Eq. (24) and is independent of ϵ (Fig. 1). Near $\alpha = 2$, corrections due to the finite resolution are noticeable, but the numerics clearly show that the variance of the distribution $P(u_\alpha)$ decreases as $\epsilon \to 0$.

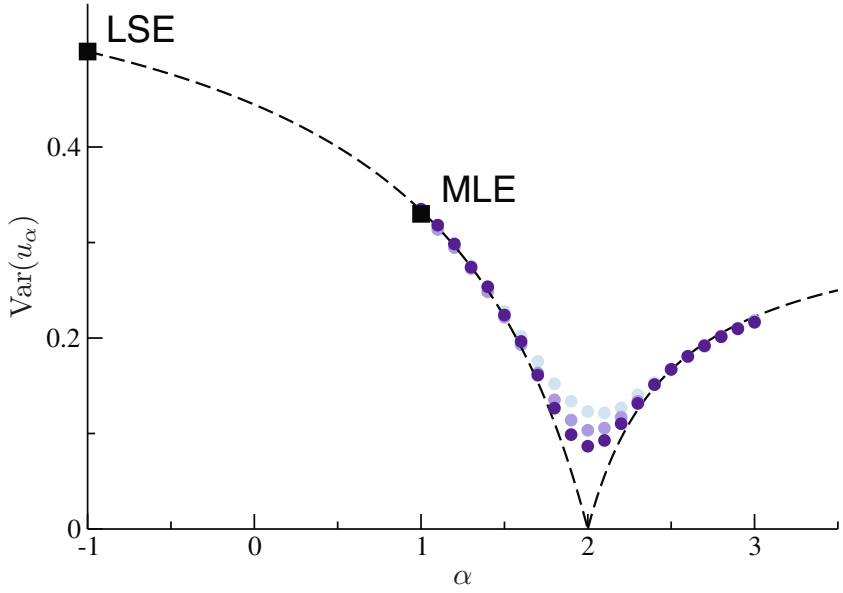

Fig. 1. Variance of the distribution $P(u_\alpha)$ for different values of α. The dashed curves correspond to Eq. (24). The symbols correspond to the values obtained from numerical simulations of 3D random walks for (from light to dark) $\epsilon = 5 \times 10^{-5}$ (●), 5×10^{-6} (●) and 5×10^{-7} (●). The solid squares correspond to the values for Var $[u_{-1}]$ (LSE) and Var $[u_1]$ (MLE) as indicated by the labels.

We now turn our attention to the distribution function $P(u_\alpha)$, which is obtained by inverting the Laplace transform in Eq. (15) with respect to the parameter σ:

$$P(u_\alpha) = \frac{1}{2\pi i} \int_{\gamma - i\infty}^{\gamma + i\infty} d\sigma \, \exp\left(\sigma u_\alpha\right) \, \Phi(\sigma) \,, \tag{25}$$

where γ is a real number chosen in such a way that the contour path of integration is in the region of convergence of $\Phi(\sigma)$. Since for $\alpha \neq 2$ all the poles of the moment-generating function lie on the complex plane on the negative real σ-axis [36,37], we can set $\gamma = 0$ in (25) and find, to leading order in ϵ

$$P(u_\alpha) = \frac{1}{\pi} \int_0^\infty \frac{dz \, \cos\left(z u_\alpha - d \, \phi_\alpha(z)/2\right)}{\rho_\alpha^{d/4}(z)}, \tag{26}$$

where, for $\alpha < 2$,

$$\rho_\alpha(z) = \Gamma^2(\nu) \left(\frac{\chi_1}{z}\right)^{\nu - 1} \left[\mathrm{ber}_{\nu-1}^2 \left(2\sqrt{\frac{z}{\chi_1}} \right) + \mathrm{bei}_{\nu-1}^2 \left(2\sqrt{\frac{z}{\chi_1}} \right) \right], \tag{27}$$

and the phase ϕ is given by

$$\phi_\alpha(z) = \mathrm{arctg} \left[\mathrm{ber}_{\nu-1} \left(2\sqrt{\frac{z}{\chi_1}} \right) \mathrm{ber}_{\nu-1}^{-1} \left(2\sqrt{\frac{z}{\chi_1}} \right) \right], \tag{28}$$

while for $\alpha > 2$ we have

$$\rho_\alpha(z) = \Gamma^2(1 - \nu) \left(\frac{\chi_2}{z}\right)^{-\nu} \left[\mathrm{ber}_{-\nu}^2 \left(2\sqrt{\frac{z}{\chi_2}} \right) + \mathrm{bei}_{-\nu}^2 \left(2\sqrt{\frac{z}{\chi_2}} \right) \right], \tag{29}$$

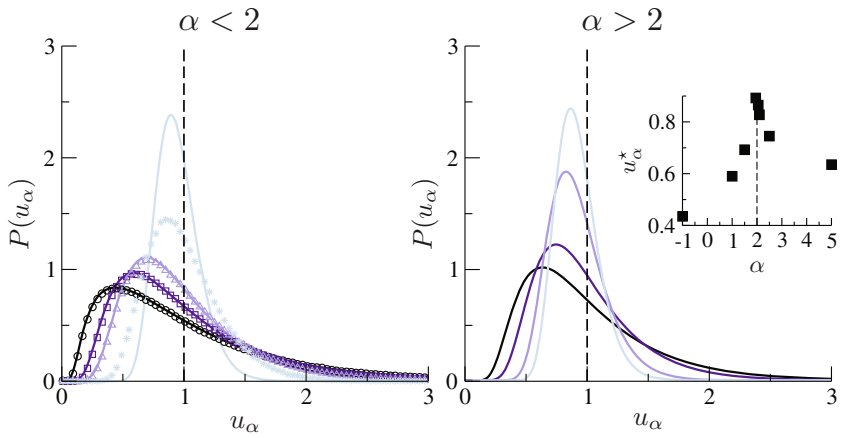

Fig. 2. The distribution $P(u_\alpha)$ for different $\alpha \neq 2$ in three dimensions. The curves from the left to the right (darker to lighter) in the left panel correspond to $\alpha = -1$ (LSE), $\alpha = 1$ (MLE), $\alpha = 3/2$ and $\alpha = 1.95$ (blue), and in the right panel to $\alpha = 5$, $\alpha = 3$, $\alpha = 2.5$ and $\alpha = 2.05$. The symbols in the left panel correspond to numerical simulations of random walks in three dimensions. In the inset we show the most probable value $u^\star_\alpha$ as a function of α.

Table 1. Most probable value $u^\star_\alpha$ and variance of the normalized estimator u_α, for different values of α and $\epsilon \to 0$.

Estimator	$u^\star_\alpha$	$\mathrm{Var}(u_\alpha)$
LSE u_{-1}	≈ 0.44	0.5
MLE u_1	≈ 0.6	≈ 0.33
Weighted BM $u_{1.95}$	≈ 0.94	≈ 0.032

and

$$\phi_\alpha(z) = \mathrm{arctg}\left[\mathrm{ber}_{-\nu}\left(2\sqrt{\frac{z}{\chi_2}}\right)\mathrm{ber}^{-1}_{-\nu}\left(2\sqrt{\frac{z}{\chi_2}}\right)\right], \tag{30}$$

where $\mathrm{ber}_\mu(x)$ and $\mathrm{bei}_\mu(x)$ are the Kelvin functions [39].

In Figs. 2 we plot $P(u_\alpha)$ in Eq. (26) for three-dimensional systems. Indeed, the most probable value $u^\star \to 1$ when $\alpha \to 2$ either from above or from below. Note that for any exponent $\alpha \neq 2$, $u^\star$ is smaller than the average value 1. Nevertheless, already for $\alpha = 1.95$ (or $\alpha = 2.05$) we get the most probable value $u^\star \approx 0.94$, which outperforms the LSE ($u^\star \approx 0.44$) and the MLE ($u^\star \approx 0.6$). For $\alpha = 1.95$ the variance $\mathrm{Var}(u_\alpha) \approx 0.032$, which is an order of magnitude less than the variances observed for LSE ($= 0.5$) and the MLE (≈ 0.33). Similarly to Fig. 1, finite-resolution corrections are negligible for $\alpha < 1.5$ and $\alpha > 2.5$, and $P(u_\alpha)$ is well described by Eq. (20). For $\alpha = 1.95$ and finite resolution $\epsilon = 10^{-7}$, we obtain a broader distribution and with a smaller u^* than the corresponding to Eq. (20) for infinite resolution. Note, however, that the most probable value of $P(u_{1.95})$ that we obtain at finite resolution is ≈ 0.84, which outperforms the LSE and MLE for infinite resolution. As a matter of fact, it is evident from Fig. 1 that for any finite resolution, at least $< 5 \times 10^{-5}$, the variance of the weighted LSE u_α outperforms the unweighted LSE and MLE at infinite resolution. A comparison between LSE, MLE and our weighted LSE is shown in Table 1.

When $\alpha = 2$ and $\epsilon = t_0/T$ small but finite we consider a slightly more general form for $\omega(t)$:

$$\omega(t) = \begin{cases} 2\xi/t_0^2, & \text{for } t < t_0, \\ 1/t^2, & \text{for } t_0 \le t \le T, \end{cases} \tag{31}$$

where ξ is a tunable amplitude. For such a choice, the moment generating function is given explicitly by [36]

$$\Phi(\sigma) = \left(\frac{2\,\delta\,\epsilon^{(\delta-1)/2}}{\phi_+} \right)^{d/2} \left[1 + \frac{\phi_-}{\phi_+}\,\epsilon^{\delta} \right]^{-d/2}, \tag{32}$$

with

$$\phi_\pm = (\delta \pm 1) \left[\mathrm{ch}\left(\sqrt{2\gamma\xi\sigma} \right) \pm \frac{\delta \mp 1}{2\sqrt{2\gamma\xi\sigma}} \mathrm{sh}\left(\sqrt{2\gamma\xi\sigma} \right) \right], \tag{33}$$

where $\delta = \sqrt{1 + 4\gamma\sigma}$ and $\gamma = 2/d(\xi + \ln(1/\epsilon))$. Differentiating Eq. (32), we find

$$\mathrm{Var}[u_2] = \frac{4}{3d}\, \frac{3\ln(1/\epsilon) - 3(1-\epsilon) + 2(1-\epsilon)\xi + \xi^2}{(\xi + \ln(1/\epsilon))^2}\,. \tag{34}$$

Now it is required to minimize (34) with respect to ξ. We note first that $\mathrm{Var}(u_2)$ is a non-monotonic function of ξ. However, we find that the optimal value of ξ is, for arbitrary ϵ

$$\xi = \xi_{\mathrm{opt}} = \frac{(2+\epsilon)\ln(1/\epsilon) - 3(1-\epsilon)}{\ln(1/\epsilon) + \epsilon - 1}\,. \tag{35}$$

This function and its optimal value are shown in Fig. 3. Therefore, corresponding optimized variance is

$$\mathrm{Var}_{\mathrm{opt}}(u_2) = \frac{4}{3d}\, \frac{3\ln(1/\epsilon) - 4 + 5\epsilon - \epsilon^2}{\ln(1/\epsilon)\,(\ln(1/\epsilon) + 1 + 2\epsilon) - 3(1-\epsilon)}\,. \tag{36}$$

From Eq. (36) we find that in $3d\ \mathrm{Var}_{\mathrm{opt}}(u_2) \approx 0.144,\ 0.096,\ 0.082$ for $\epsilon = 10^{-3}$, 10^{-5}, 10^{-6}, respectively. When $\epsilon \to 0$, $\mathrm{Var}_{\mathrm{opt}}(u_2)$ vanishes as

$$\mathrm{Var}_{\mathrm{opt}}(u_2) \sim \frac{4}{d}\frac{1}{\ln(1/\epsilon)}\,. \tag{37}$$

Therefore, $\mathrm{Var}_{\mathrm{opt}}(u_2)$ can be made arbitrarily small but at expense of a progressively higher resolution. In the limit $\epsilon \to 0$ the distribution converges to a delta-function. The estimators with $\alpha = 2$ are the only, in the family defined by Eq. (10), that possess this ergodic property.

5 Diffusion in the presence of a random potential

In this section we consider a Brownian motion in a one-dimensional inhomogeneous energy landscape, where the disorder is correlated over a finite length ξ_c. This model gives a simple description of diffusion of a protein along a DNA sequence, for instance, where the particle interacts with several neighboring base pairs at a time [38]. The total binding energy of the protein is assumed to be a random variable. When the particle hops one neighboring base further to the right or to the left, its new energy is highly correlated to the value it had before the jump. Slutsky *et al.* [38] modeled this process as a point-like particle diffusing on a one-dimensional lattice of unit spacing

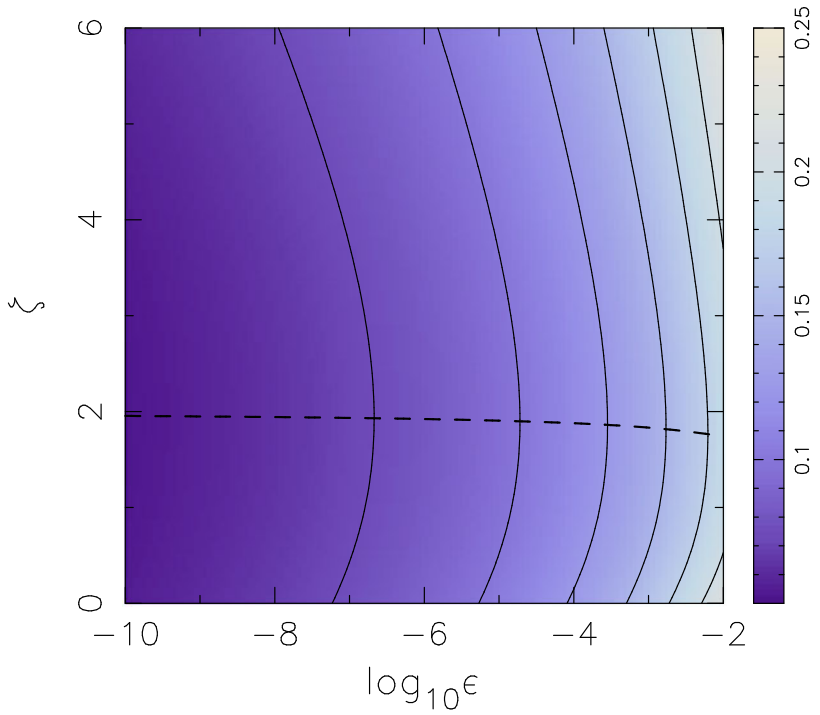

Fig. 3. Colour density plot of $\mathrm{Var}[u_2]$ as a function of ξ and ϵ. The dashed curve corresponds to ξ_{opt} of Eq. (35), and thus, to the optimal value of $\mathrm{Var}[u_2]$ for fixed ϵ.

with random site energies $\{U_i\}$, whose distribution is Gaussian with zero mean, variance η^2 and is correlated in space as $\langle (U_i - U_j)^2 \rangle = 2\eta^2[1-\exp(-|i-j|/\xi_c)]$, where ξ_c is a correlation length. At each time step, the particle located at some site i jumps to the left or to the right with probabilities $p_i \propto \exp[\beta(U_i - U_{i-1})]$ and $q_i \propto \exp[\beta(U_i - U_{i+1})]$, respectively, where $p_i + q_i = 1$. Diffusion is asymptotically normal for any disorder strength η. Nevertheless, the particle can be trapped in local energy minima for long periods of time. During an extended intermediate time regime, it is observed that first passage properties fluctuate widely from one sample to another [38].

In [32], we studied the probability distribution function $P(u_\alpha)$ with $\alpha = 1$ for a Brownian particle moving in such a disordered potential. There we found that $P(u_0)$ is strongly affected by the strength of the disorder and indeed, the presence of disorder with short-ranged correlations tends to broaden the distribution of the measured D, as it presents an additional source of fluctuations.

Here we generalise the study in [32] to different values of α. In Fig. 4 we show numerical results for the variance $\mathrm{Var}\,[u_\alpha]$ for a Brownian particle moving on a disordered potential for different disorder strengths η and different precision ϵ. As expected, for a fixed ϵ, the variance grows in proportion with the disorder strength η. We do not expect that for these dynamics u_2 will be an ergodic estimator of the diffusion coefficient and as a matter of fact, we cannot say *a priori*, that there exists a value α for which u_α is ergodic in this case. Nevertheless, it is interesting to note in Fig. 4 that the variance of u_α gets smaller around some value $\alpha = \alpha^\star$. Moreover, apparently $\alpha^\star \to 2$ as $\eta \to 0$. This behaviour is more evident in Fig. 5 where we show the dependence of $\mathrm{Var}\,[u_\alpha]$ on α for a fixed precision $\epsilon = 10^{-6}$ and different strengths of the disorder η. As before, $\mathrm{Var}\,[u_\alpha]$ seems to attain a minimum for a value of α which moves toward 2 as $\eta \to 0$. A rough estimation of the optimal value $\alpha^\star$ from the

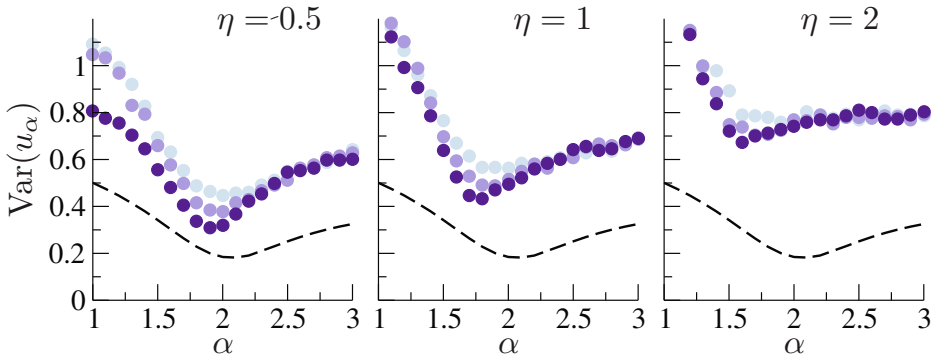

Fig. 4. Variance Var $[u_\alpha]$ for a Brownian particle moving on a short range disordered potential, as a function of α for different values of precision: $\epsilon = 10^{-4}$ (●), 10^{-5} (●) and 10^{-6} (●). Each panel corresponds to different disorder strengths as indicated by the labels, and $\beta = 1$. The dashed curve corresponds to the pure Brownian motion ($\eta = 0$) for $\epsilon = 10^{-6}$.

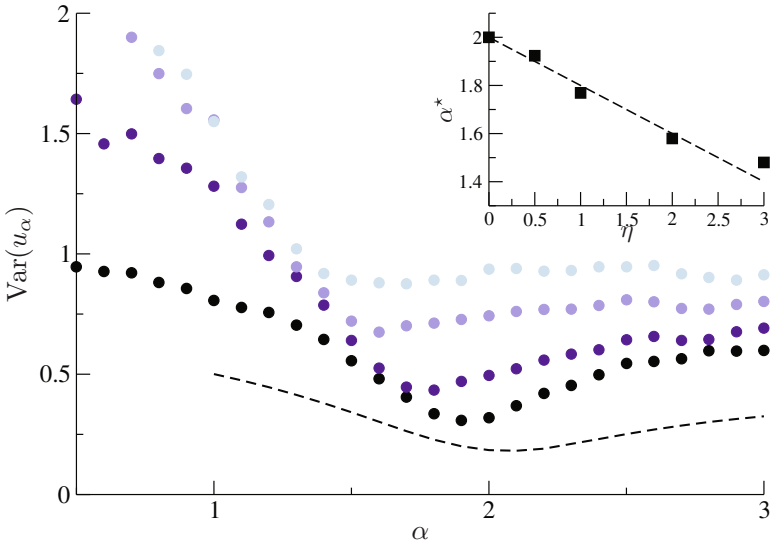

Fig. 5. Variance Var $[u_\alpha]$ for a Brownian particle moving on a disordered potential, as a function of α for $\epsilon = 10^{-6}$ and different values of the disorder strength: $\eta = 3$ (●), 2 (●), 1 (●) and 0.5 (●). The dashed curve corresponds to the pure Brownian motion ($\eta = 0$). In the inset, a rough estimation of the optimal $\alpha^\star$ as a function of η. The dashed curve corresponds to $\alpha^\star = 2 - \eta/5$.

numerical data, shows that the dependence of $\alpha^\star$ on η is consistent with the affine law $\alpha^\star = 2 - \eta/5$, as shown in the inset of Fig. 5.

Finally, to highlight the role of the trajectory-to-trajectory fluctuations, we consider the probability density function $P(\omega_\alpha)$ of the random variable

$$\omega_\alpha = \frac{u_\alpha^{(1)}}{u_\alpha^{(1)} + u_\alpha^{(2)}}\,, \tag{38}$$

where $u_\alpha^{(1)}$ and $u_\alpha^{(2)}$ are two identical independent random variables with the same distribution $P(u_\alpha)$. The distribution $P(\omega_\alpha)$, introduced recently in [19] (see also [40–42]),

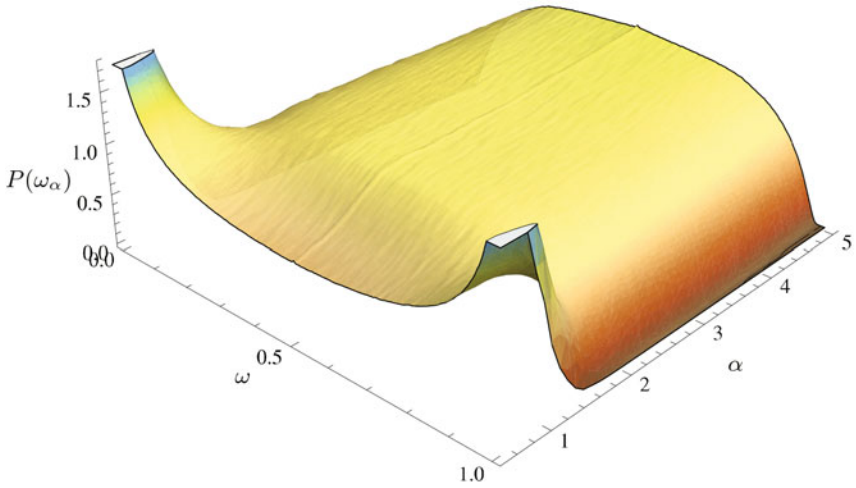

Fig. 6. Distribution $P(\omega_\alpha)$ as a function of ω and α, for fixed disorder strength $\eta = 3$ and $\epsilon = 10^{-5}$. The colour ramp increases from red (small values) to blue (large values).

is a robust measure of the effective broadness of $P(u_\alpha)$, which *probes* the likelihood of the event that the diffusion coefficients drawn from two different trajectories are equal to each other. This characteristic property can be readily obtained via an expression [43]

$$P(\omega_\alpha) = \frac{1}{(1-\omega_\alpha)^2} \int_0^\infty u\, du\, P(u)\, P\left(\frac{\omega_\alpha}{1-\omega_\alpha} u\right). \tag{39}$$

Hence, $P(\omega_\alpha)$ is known once we know $P(u_\alpha)$.

In [32], we observed in the case $\alpha = 1$ that for $\eta \approx 0.8$ the distribution $P(\omega_1)$ undergoes a continuous shape reversal transition – from a unimodal bell-shaped form to a characteristic bimodal M-shape one with the minimum at $\omega_1 = 1/2$ and two maxima approaching 0 and 1 at larger disorder strengths. Therefore, indicating that for $\eta > 0.8$ sample-to-sample fluctuations becomes essential and it is most likely that the diffusion coefficients drawn from two different trajectories will be different. Here we have computed the distribution $P(\omega_\alpha)$ for different values of α, η and ϵ. We have found that the transition of $P(\omega_\alpha)$ described above, is robust with respect to α. Furthermore, we have also found that the same transition occurs for fixed strength of the disorder and varying α. An example of this transition is shown as a surface plot in Fig. 6. For $\eta = 3$, the transition from bimodal to unimodal $P(\omega_\alpha)$ occurs around $\alpha \approx 2$. This means that in the presence of disorder, among the estimators (10), those for smaller α present more trajectory-to-trajectory fluctuations than those with larger α.

6 Conclusions

To summarize, we have discussed different statistical estimators of the diffusion coefficient of a single (or few) Brownian single-particle trajectories. We have differentiated between one-time and two-time estimators. In the case of the former, we have discussed a family of weighted least-squares estimators and showed that for standard Brownian motion there exist a unique representative of this family u_2 that possesses the ergodic property, meaning that the estimated diffusion coefficient converges to its true value in the limit of infinite precision $\epsilon \to 0$.

Moreover, we have sketched the derivation of the full probability distribution function of u_α in the leading order in ϵ. For $\alpha = 2$, we have extracted the optimal value of the variance as a function of the precision ϵ, and shown that in the limit $\epsilon \to 0$, $\mathrm{Var}\,[u_e]$ vanishes in proportion of $1/\ln(T)$. This means that for practical purposes the methods based on two-time correlation functions can provide better estimators, because the variance of the corresponding estimator decays faster, as $1/T$, even in the presence of localization errors [23–26].

Furthermore, we studied trajectories of a Brownian particle moving in a random potential with short-ranged correlations. Our numerical results suggest that there exist an optimal value $\alpha = \alpha^\star$ for which the variance of u_α is minimal. We found that $\alpha^\star$ converges to 2 inversely proportionally to the strength of the disorder η. Moreover, we found that the trajectory-to-trajectory fluctuations increase in proportion to η and are inversely proportional to α. This means that a robust estimator of the diffusion coefficient for the random motion in disordered potentials is that for which the short time dynamics is more efficiently emphasized. The question on the existence of an ergodic estimator of the diffusion coefficient for disordered potentials deserves further investigation.

CMM is partially supported by the European Research Council and the Academy of Finland.

References

1. J. Perrin, C.R. Acad. Sci. **146**, 967 (1908)
2. J. Perrin, Ann. Chim. Phys. **18**, 5 (1909)
3. C. Bräuchle, D.C. Lamb, J. Michaelis (eds.), *Single particle tracking and single molecule energy transfer* (Wiley-VCH, Weinheim, 2010)
4. M.J. Saxton, K. Jacobson, Ann. Rev. Biophys. Biomol. Struct. **26**, 373 (1977)
5. T.G. Mason, D.A. Weitz, Phys. Rev. Lett. **74**, 1250 (1995)
6. W.J. Greenleaf, M.T. Woodside, S.M. Block, Annu. Rev. Biophys. Biomol. Struct. **36**, 171 (2007)
7. S.C. Weber, A.J. Spakowitz, J.A. Theriot, Phys. Rev. Lett. **104**, 238102 (2010)
8. I. Bronstein, et al., Phys. Rev. Lett. **103**, 018102 (2009)
9. G. Seisenberger, et al., Science **294**, 1929 (2001)
10. A.V. Weigel, B. Simon, M.M. Tamkun, D. Krapf, Proc. Natl. Acad. Sci. USA **108**, 6438 (2011)
11. I. Golding, E.C. Cox, Phys. Rev. Lett. **96**, 098102 (2006)
12. M.J. Saxton, Biophys. J. **72**, 1744 (1997)
13. T. Pederson, Nature Cell Biol. **2**, E73 (2000)
14. A. Rebenshtok, E. Barkai, Phys. Rev. Lett. **99**, 210601 (2007)
15. J.H. Jeon, et al., Phys. Rev. Lett. **106**, 048103 (2011)
16. Y. He, S. Burov, R. Metzler, E. Barkai, Phys. Rev. Lett. **101**, 058101 (2008)
17. A. Lubelski, I.M. Sokolov, J. Klafter, Phys. Rev. Lett. **100**, 250602 (2008)
18. J. Schulz, E. Barkai, R. Metzler, Ageing effects in single particle trajectory averages [arXiv:1204.0878v1]
19. C. Mejía-Monasterio, G. Oshanin, G. Schehr, J. Stat. Mech., P06022 (2011)
20. T.G. Mattos, C. Mejía-Monasterio, R. Metzler, G. Oshanin, Phys. Rev. E **86**, 031143 (2012)
21. Y.M. Wang, R.H. Austin, E.C. Cox, Phys. Rev. Lett. **97**, 048302 (2006)
22. M. Goulian, S.M. Simon, Biophys. J. **79**, 2188 (2000)
23. A.J. Berglund, Phys. Rev. E **82**, 011917 (2010)
24. X. Michalet, Phys. Rev. E **82**, 041914 (2010)
25. X. Michalet, Phys. Rev. E **83**, 059904 (2011)
26. X. Michalet, A.J. Berglund, Phys. Rev. E **85**, 061916 (2012)

27. D.S. Grebenkov, Phys. Rev. E **83**, 061117 (2011)
28. D.S. Grebenkov, Phys. Rev. E **84**, 031124 (2011)
29. A. Andreanov, D.S. Grebenkov, J. Stat. Mech., P07001 (2012)
30. V. Tejedor, et al., Biophys J **98**, 1364 (2010)
31. D. Boyer, D.S. Dean, J. Phys. A: Math. Gen. **44**, 335003 (2011)
32. D. Boyer, D.S. Dean, C. Mejía-Monasterio, G. Oshanin, Phys. Rev. E **85**, 031136 (2012)
33. H. Qian, M.P. Sheetz, E.L. Elson, Biophys. J. **60**, 910 (1991)
34. D. Martin, M. Forstner, J. Käs, Biophys. J. **83**, 2109 (2002)
35. T. Savin, P.S. Doyle, Biophys. J. **88**, 623 (2005)
36. D. Boyer, D.S. Dean, C. Mejía-Monasterio, G. Oshanin [arXiv:1211.1151]
37. D. Boyer, D.S. Dean, C. Mejía-Monasterio, G. Oshanin (to be published)
38. M. Slutsky, M. Kardar, L.A. Mirny, Phys. Rev. E **69**, 061903 (2004)
39. M. Abramowitz, I.R. Stegun (eds.), *Handbook of mathematical functions* (Dover, New York 1972)
40. I. Eliazar, Physica A **356**, 207 (2005)
41. I. Eliazar, I.M. Sokolov, J. Phys. A: Math. Theor. **43**, 055001 (2010)
42. I. Eliazar, I.M. Sokolov, Physica A **391**, 3043 (2012)
43. C. Mejía-Monasterio, G. Oshanin, G. Schehr, Phys. Rev. E **84**, 035203 (2011)